

Pulmonary Bioassay Studies with Nanoscale and Fine-Quartz Particles in Rats: Toxicity is Not Dependent upon Particle Size but on Surface Characteristics

David B. Warheit,^{*,1} Thomas R. Webb,^{*} Vicki L. Colvin,[†] Kenneth L. Reed,^{*} and Christie M. Sayes^{*}

^{*}DuPont Haskell Laboratory for Health and Environmental Sciences, Newark, Delaware 19714-0050; and

[†]Department of Chemistry, Rice University, Houston, TX 77005

Received August 13, 2006; accepted September 26, 2006

Pulmonary toxicology studies in rats demonstrate that nanoparticles are more toxic than fine-sized particles of similar chemistry. This study, however, provides evidence to contradict this theory. The aims of the study were (1) to compare the toxicity of synthetic 50 nm nanoquartz I particles versus (mined) Min-U-Sil quartz (~500 nm); the toxicity of synthetic 12 nm nanoquartz II particles versus (mined) Min-U-Sil (~500 nm) versus (synthetic) fine-quartz particles (300 nm); and (2) to evaluate the surface activities among the samples as they relate to toxicity. Well-characterized samples were tested for surface activity and hemolytic potential. In addition, groups of rats were instilled with either doses of 1 or 5 mg/kg of carbonyl iron (CI) or various α -quartz particle types in phosphate-buffered saline solution and subsequently assessed using bronchoalveolar lavage fluid biomarkers, cell proliferation, and histopathological evaluation of lung tissue at 24 h, 1 week, 1 month, and 3 months postexposure. Exposures to the various α -quartz particles produced differential degrees of pulmonary inflammation and cytotoxicity, which were not always consistent with particle size but correlated with surface activity, particularly hemolytic potential. Lung tissue evaluations of three of the quartz samples demonstrated “typical” quartz-related effects—dose-dependent lung inflammatory macrophage accumulation responses concomitant with early development of pulmonary fibrosis. The various α -quartz-related effects were similar qualitatively but with different potencies. The range of particle-related toxicities and histopathological effects in descending order were nanoscale quartz II = Min-U-Sil quartz > fine quartz > nanoscale quartz I > CI particles. The results demonstrate that the pulmonary toxicities of α -quartz particles appear to correlate better with surface activity than particle size and surface area.

Key Words: α -quartz particles; pulmonary toxicity; nanoscale quartz particles; particle size; particle characterization; surface activity.

Pulmonary toxicity studies in rats demonstrate that low solubility ultrafine particles (generally consistent with the term “nanoparticles” and defined as particles in the size range ≤ 100 nm) produce more potent inflammatory responses when compared to larger particles of similar chemistry at the same mass concentrations or doses (Donaldson *et al.*, 2001a; Oberdorster *et al.*, 2005). Along with particle size, surface area and particle number characteristics appear to be integral components in contributing to the mechanisms of ultrafine particle-related lung toxicity. Assumed to be important in this lung inflammatory process is the very high size-specific deposition rate of ultrafine particulates when inhaled experimentally as singlet ultrafine particles rather than as aggregated particles. Some evidence suggests that inhaled ultrafine particles, after deposition in the lung, largely escape alveolar macrophage surveillance and gain greater access to the pulmonary interstitium through translocation from alveolar spaces through epithelium (Donaldson *et al.*, 2001a; Oberdorster *et al.*, 2005).

Recently, we compared the pulmonary toxicity effects of intratracheally instilled nanoscale TiO₂ dots and rods with low toxicity, reference particle type, fine-sized TiO₂ particles (~300 nm). No significant differences in lung toxicity indices were measured in the evaluations of nanoscale versus fine-sized TiO₂ particles. The results with TiO₂ nanoscale rods and nanoscale dots were considered to be at variance with the “conventional wisdom” that nanoscale particles are always more toxic than fine-sized particulates of similar chemical composition. Accordingly, it was concluded that these findings run counter to the postulation that surface area is the major factor associated with the pulmonary toxicity of nanoscale particle types (Warheit *et al.*, 2006).

The concept of correlating particle size and surface area with pulmonary inflammation has traditionally been applied to low solubility/low toxicity particulates, often under particle overload conditions in the lungs of exposed rats. What has not been addressed or systematically investigated are the influences of particle size and surface area with lung inflammatory responses when assessing the mechanisms of toxicity of *cytotoxic*

¹ To whom correspondence should be addressed at DuPont Haskell Lab, 1090 Elkton Rd., PO Box 50, Newark, DE 19714-0050. Fax: (302) 366-5207. E-mail: david.b.warheit@usa.dupont.com.

particulates such as α -quartz particles. Donaldson and colleagues have suggested that the surface activity of quartz particles plays an important role in determining its toxic effects when inhaled. In this regard, these investigators have proposed that the hazard posed by quartz is not a constant or consistent entity but is dependent upon the origin of the silica sample or its contact with other chemicals/minerals within its complex composition. The surface activity generally facilitates the ability of quartz particles to generate free radicals and cause oxidative stress in biological systems (Razzaboni and Bolsaitis, 1990). However, these features are not uniform among all of the quartz samples evaluated. Thus, based on the results of their studies, Donaldson *et al.* (2001b) have concluded that quartz cannot be dealt with as a single hazard entity, in contrast to most other dusts.

The aim of this study was to assess the role of particle size/surface area as well as surface activity of differential α -quartz particle types to produce pulmonary inflammatory and adverse tissue effects in rats. To test this hypothesis, we have synthesized and characterized nanoscale and fine α -quartz particulates of various sizes. Moreover, following instillation of particles into the lungs of rats, we have compared the potency of

inflammation and cytotoxic lung effects of nano or fine α -quartz particle types at equivalent mass doses with a standard active reference α -quartz particle type, Min-U-Sil 5. In addition, we have assessed the surface activity of the quartz particle types and correlated these effects with *in vivo* pulmonary endpoints.

MATERIALS AND METHODS

General Experimental Design

The general approach to this study was to conduct substantial particle characterization assessments of the quartz particulates, concomitant with particle surface activity studies (electron spin resonance [ESR] and hemolytic potential) and *in vivo* pulmonary bioassay studies following intratracheal instillation of particulates in male rats.

Particle Types

Min-U-Sil α -quartz particles (crystalline silica, Min-U-Sil 5) ranging in size from 300 nm to 2 μ m were obtained from U.S. Silica Co., Berkeley Springs, WV (see Fig. 1 and Table 1). The nano I and II and fine α -quartz particles were synthesized hydrothermally as described below at the Center for Biological and Environmental Nanotechnology at Rice University, Houston, TX. Carbonyl iron (CI) particles, ranging in size from 0.8 to 3.0 μ m were obtained from GAF Corporation, Wayne, NJ.

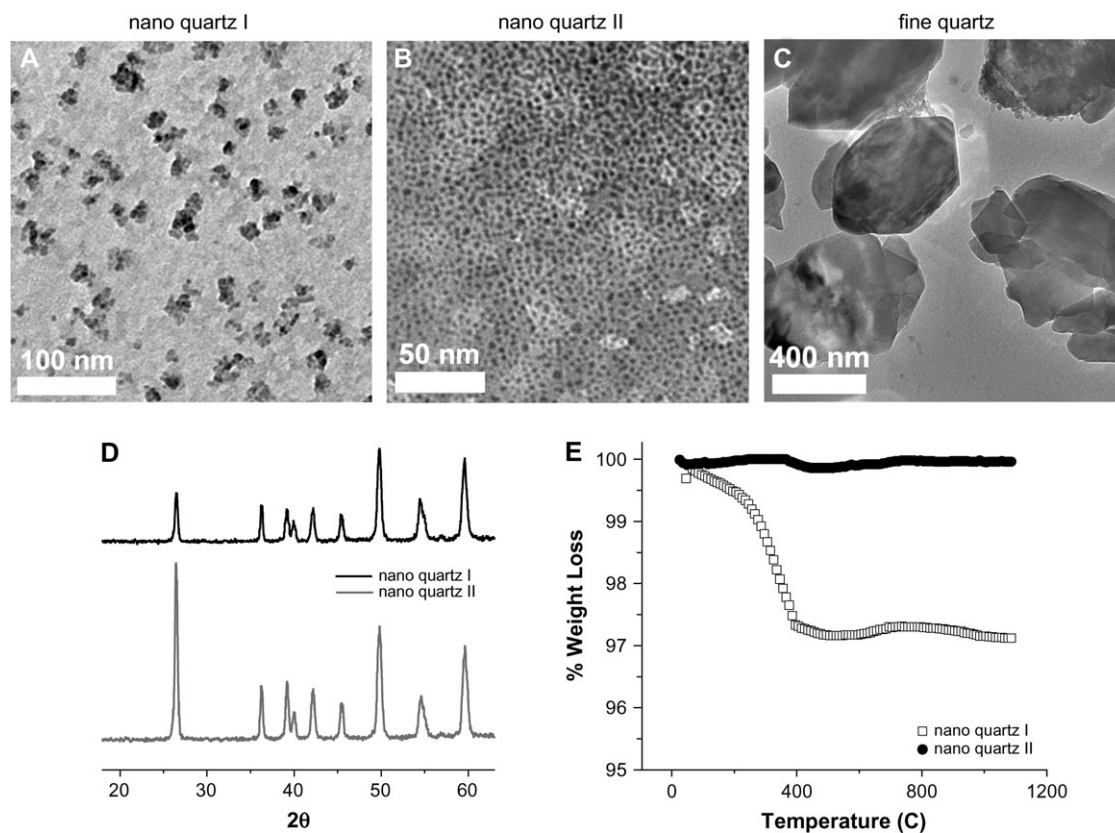


FIG. 1. α -Quartz characterization. The characterization of nanoquartz I, nanoquartz II, and fine-quartz samples used in the two intratracheal instillation studies described here. (A) Transmission electron micrograph of the nanoquartz sample used in study #1. (B, C) TEMs of the nanoquartz and fine-quartz samples used in study #2. (D) XRD pattern of the two different nanoquartz samples. (E) DTA of the nanoquartz sample used in study #2. The DTA weight loss profile shows loss of residual water at 100°C and burn-off of small molecular weight organic containments at 500°C. Sizing data were obtained using TEM and scanning electron microscope, and DLS.

TABLE 1
 α -Quartz Particle Characterization

Sample	Average size (nm)	Size range (nm)	Surface area (m ² /g)	Crystallinity	ICP-AES (% Fe content)
Nanoquartz I	50	30–65	31.4	α -Quartz	0.080%
Nanoquartz II	12	10–20	90.5	α -Quartz	0.034%
Fine quartz	300	100–500	4.2	α -Quartz	0.011%
Min-U-Sil	534	300–700	5.1	α -Quartz	0.042%

Nano and Fine α -Quartz Production and Characterization

Particle production. Nanoscale quartz particles I (50 nm), nanoscale quartz particles II (12 nm), and fine quartz (300 nm) were synthesized hydrothermally (in NaOH at 300°C) in low surfactant concentrations (Fig. 1 and Table 1). A total of 3.5 g of fumed silica was dispersed in 100 ml of a 0.1N aqueous NaOH solution and stirred in a stainless steel bomb reactor for 80 min at 300°C. The resulting suspension of nanoscale α -quartz crystals was centrifuged for 20 min at 110 \times g to separate the nanoparticles from the larger particles. The supernatant was decanted and saved in a separate centrifuge tube, while the pellet was redispersed in ultrapure Milli-Q water and centrifuged for another 20 min at 110 \times g. This sequence of decantation of supernatant, redispersion of the pellet, and recentrifugation was repeated until the pH of the dispersed pellet was \sim 8, after which the solid was vacuum dried for several hours. This “fine” solid was labeled fine quartz.

The decanted supernatants were combined and centrifuged for 20 min at 3700 \times g to obtain a pellet consisting of nanoscale quartz crystals. The resulting supernatant was decanted, while the pellet was redispersed in MilliQ water and centrifuged for another 20 min at 3700 \times g. This sequence of decantation of supernatant, redispersion of the pellet, and recentrifugation was repeated until the pH of the dispersed pellet was \sim 8, after which the solid was vacuum dried for several hours. This “nano” solid was labeled nanoquartz I. The experiment was repeated to produce nanoquartz II. Even though the same synthesis procedures were utilized for the preparation of both nanoquartz I and nanoquartz II samples, minor changes in reaction conditions affected the product. Specifically, when producing nanocrystalline materials via a solvothermal treatment, the size, shape, and crystal structure of the crystallite are sensitive functions of the starting material and surfactant concentrations, as well as temperature, pressure, and reaction time. Of the various properties of quartz nanoparticles, size is the most sensitive and most difficult property to reproduce. Because these two samples (I and II) were produced in two separate batches, slight changes in reactant concentrations and reaction conditions easily led to the formation of two different sized nanoquartz particle types. The shape and crystal structure, however, remained identical.

All resulting powders were sterilized by autoclaving for 30 min at 120°C. The two nanoquartz samples (I and II) were prepared separately to provide a fresh sample for the *in vivo* pulmonary exposure. Because of this, small inconsistencies within the nanocrystalline preparation resulted in variable samples. A detailed discussion of the differences in the two nanoquartz samples is presented below (see Results).

Particle Characterization

Each sample was characterized using a variety of physio-chemical techniques. These techniques included cryogenic transmission electron microscopy, (cryo-TEM), dynamic light scattering (DLS), Brunauer-Emmett-Teller specific surface area analysis (BET SSA), X-ray diffraction (XRD), differential thermal analysis (DTA), inductively coupled plasma atomic emission spectrophotometry (ICP-AES), and ESR.

Cryo-transmission electron micrographs were taken on a JEOL 2010 microscope. Each TEM sample was prepared by flash freezing 2 μ l of 3 mg/ml nano

or fine-quartz suspension via FEI Vitrobot at liquid nitrogen temperature (-196°C) onto a 300 mesh copper/carbon grid (Ted Pella Inc., Redding, CA).

DLS analysis was performed using Malvern Zetasizer Nano-S, model Zen1600. Sizing data were taken on each particle sample in phosphate-buffered saline (PBS) solution.

BET-SSAs were determined from N₂ adsorption onto the nanoscale and fine-quartz powders using a Micrometrics ASAP 2010 apparatus (Brunauer *et al.*, 1938). Samples were degassed for several hours prior to the N₂ adsorption analysis, which was carried out at liquid nitrogen temperature (-196°C).

XRD patterns were collected using a Siemens Platform-Model General Area Detector Diffraction System with a Cu K α source. The powder samples were run with an internal silicon powder standard to account for instrumental line broadening when calculating grain sizes from the α -quartz line widths. Profiles were used to determine purity, crystal structure, and crystallite size (Otwinowski and Minor, 1997).

DTA was performed in air on a Thermal Advantage SDT 2960 apparatus using a temperature range of 25–600°C and a heating rate of 20°C/min.

ICP-AES analysis was conducted on a Varian Vista AX. Since metal impurities can alter the chemical toxicity of materials, elemental analysis is pertinent in identifying contaminants. ICP-AES is one of the most powerful analytical tool for determining the presence of metals.

General Experimental Design for Pulmonary Bioassay Studies

The fundamental features of this pulmonary bioassay are (1) low and high dose response evaluation, and (2) time course assessments to determine the sustainability of any observed effect. Thus, the major endpoints of this study were the following: (1) time course and low or high dose/response intensity of pulmonary inflammation and cytotoxicity; (2) airway and lung parenchymal cell proliferation; and (3) histopathological evaluation of lung tissue.

Two separate pulmonary bioassay experiments were conducted. In the first experiment, the effects of instilled nanoquartz I particles (50 nm) were compared to Min-U-Sil quartz particles (534 nm) or PBS solution. The pulmonary inflammatory and cytotoxic effects were assessed using bronchoalveolar lavage (BAL) evaluations. In the second experiment, the effects of intratracheally instilled nanoquartz II (12 nm) and fine-quartz particles (300 nm) were compared with Min-U-Sil quartz particles (534 nm), CI particles (negative particle control), or PBS. The endpoints measured in this experiment were pulmonary inflammation and cytotoxicity indices, airway and lung parenchymal cell proliferation, and pulmonary histopathological effects.

In the first study, groups of rats (five rats per group per dose per time point) were intratracheally instilled with doses of 1 or 5 mg/kg of nanoquartz I (50 nm) or Min-U-Sil quartz particles (534 nm). All particles were prepared in a volume of PBS and subjected to polytron dispersement. Groups of PBS-instilled rats served as controls. The lungs of PBS, and particle-exposed rats were evaluated by BAL fluid analyses at 24 h, 1 week, 1 month and 3 months postexposure (pe).

In the second study, groups of rats (five rats per group per dose per time point) were intratracheally instilled with doses of 1 or 5 mg/kg of CI particles (reference control), nanoquartz II (12 nm), Min-U-Sil quartz particles (534 nm), or fine-quartz particles (300 nm). All particles were prepared in a volume of PBS and subjected to polytron dispersement. Groups of PBS-instilled (0.5 ml) rats served as controls. The lungs of PBS, and particle-exposed rats were evaluated by BAL fluid analyses and lung tissue evaluations at 24 h, 1 week, 1 month and 3 months pe.

For the morphological studies (second study only), additional groups (four rats per group per high dose per time point) (four rats per group per low dose for the first two time points) of animals were instilled with the particle types listed above as well as PBS. These studies were dedicated for lung tissue analyses and consisted of cell proliferation assessments and histopathological evaluations of the lower respiratory tract.

Animals

Groups of male Crl:CD(SD)IGS BR rats (Charles River Laboratories, Inc., Raleigh, NC) were used in this study. The rats were approximately 8 weeks old

at study start (mean weights in the range of 240–310 g). All procedures using animals were reviewed and approved by the Institutional Animal Care and Use Committee, and the animal program is fully accredited by the Association for Assessment and Accreditation of Laboratory Animal Care.

Bronchoalveolar Lavage

The lungs of PBS and particle-exposed rats were lavaged with a warmed PBS solution as described previously (Warheit *et al.*, 1997). Methodologies for cell counts, differentials, and pulmonary biomarkers in lavaged fluids were conducted as reported in an earlier study (Warheit *et al.*, 1991, 1997). Briefly, the first 12 ml of lavaged fluids recovered from the lungs of PBS or particulate-exposed rats was centrifuged at $700 \times g$ for 5 min, and 2 ml of the supernatant was removed for clinical pathology evaluations. All biochemical assays were performed on BAL fluids using an Olympus AU640 Chemistry Analyzer at 340/380 nm using Olympus reagents. Lactate dehydrogenase (LDH), alkaline phosphatase (ALP), and lavage fluid protein were also measured using Olympus reagents. LDH is a cytoplasmic enzyme and is used as an indicator of cell injury. ALP activity is a measure of Type-II alveolar epithelial cell secretory activity, and increased ALP activity in BAL fluids is considered to be an indicator of Type-II lung epithelial cell toxicity. Enhanced BAL fluid protein concentrations relative to controls generally are consistent with increased transudation of vascular proteins from vasculature into the alveolar regions.

Airway and Lung Cell Proliferation Studies

These studies were designed to measure the effects of particle exposures on airway and lung parenchymal cell turnover in exposed rats following 24 h, 1 week, 1 and 3 months pe periods. Groups of particulate-exposed rats and corresponding PBS controls were pulsed 24 h after instillation, as well as 1 week, 1 or 3 months pe, with an intraperitoneal injection of 5-bromo-2'-deoxyuridine (BrdU) dissolved in a 0.5N sodium bicarbonate buffer solution at a dose of 100 mg/kg body weight. The rats were euthanized 6 h later by pentobarbital injection. Following cessation of spontaneous respiration, the trachea and lungs were infused with a neutral buffered formalin fixative at a pressure of 21 cm H₂O. After 20 min of fixation, the trachea was clamped, and the heart and lungs were carefully removed *en bloc* and immersion fixed in formalin. In addition, a 1-cm piece of duodenum (which served as a positive internal control) was removed and stored in formaldehyde. Following fixation procedures, parasagittal sections from the right cranial and caudal lobes and regions of the left lung lobes as well as the duodenal sections were dehydrated in 70% ethanol and sectioned for histology. The sections were embedded in paraffin, cut, and mounted on glass slides. The slides were stained with an anti-BrdU antibody, with an 3-amino-9-ethyl carbazole marker, and counterstained with aqueous hematoxylin. A minimum of 1000 cells per animal were counted each in terminal bronchiolar and in alveolar regions near the alveolar duct bifurcation. The selection of airways and lung parenchymal regions was random. For each treatment group, immunostained nuclei in airways (i.e., terminal bronchiolar epithelial cells) or lung parenchyma (i.e., epithelial, interstitial cells or macrophages) were counted by light microscopy at $\times 1000$ magnification (Warheit *et al.*, 1991, 1997).

Morphological/Histopathology Studies

The lungs of rats exposed to CI, α -quartz particles or PBS controls were weighed and prepared for microscopy by airway infusion fixation under pressure (21 cm H₂O) at 24 h, 1 week, 1 and 3 months pe. Sagittal sections of the left and right lungs were made with a razor blade. Tissue blocks were dissected from left, right upper, and right lower regions of the lung and were subsequently prepared for light microscopy (paraffin embedded, sectioned, and hematoxylin-eosin stained) (Warheit *et al.*, 1991, 1997).

In this model of quartz-induced pulmonary injury, the three major features are (1) lung inflammation; (2) accumulation of foamy alveolar macrophages; and (3) development of early fibrosis as evidenced by tissue thickening. For the semiquantitative morphometric studies (second study only), four rats per group per high dose at the 3-month pe time point were evaluated for incidences of alveolar macrophage accumulation and tissue thickening at BA junctions.

Longitudinal sections containing a terminal bronchiole and its associated alveolar ducts were evaluated in each of three sagittal sections from each of the four rats per group. For each BA junction unit, the criterion for detection of foamy alveolar macrophage accumulation was the following: confirmation of a minimum of seven accumulated macrophages within the associated alveolar ducts. Lung tissue thickening assessments, as a harbinger for early development of pulmonary fibrosis were also assessed and recorded.

Surface Activity Studies

ESR spectra were acquired on a Bruker EleXsys E-500 ESR spectrometer operating at X-band microwave frequency (9.3 GHz) with a super-high Q ER 4106 resonator. Approximately 0.5 g of each α -quartz sample was loaded into a 4-mm-outer diameter quartz tube in a nitrogen glove box. The sample tube was capped under nitrogen and loaded into the ESR resonator. Spectra were acquired at 100 K, with cooling effected by a liquid nitrogen accessory. Scans of the $g = 2$ region at higher microwave power (1.26 mW) were acquired with a sweep width of 500 G (1024 points over 83 s), a modulation amplitude of 0.5 G, a modulation frequency of 100 KHz, and a time constant of 41 ms. Scans at lower microwave power (0.020 mW) were acquired with a sweep width of 50 G (1024 points over 42 s), a modulation amplitude of 0.2 G, a modulation frequency of 100 KHz, and a time constant of 41 ms. An external Teslameter was active during the scans for precise measurement of the g factor. Spectra of nitrogen-filled quartz tubes were acquired under identical conditions for the purpose of baseline subtraction; this subtraction has been applied to all spectra discussed in the manuscript.

Hemolytic Potential of α -Quartz Particles

The hemolytic potentials of the four α -quartz particles used in these studies were measured based on the method of Harington *et al.* (1971). Erythrocytes were obtained from the fresh blood of a healthy human donor. The red blood cells (RBC) were washed four times by suspending in PBS solution before centrifugation at $1200 \times g$. The final suspension consisted of 4% by volume RBC suspended in PBS. Quartz was prepared as described previously and diluted in saline to give a stock solution of 30 mg/ml, then serially diluted ranging 15–0.059 mg/ml. The quartz suspensions (150 μ l) were mixed with 75 μ l of erythrocyte suspension and incubated for 30 min at 37°C. After incubation the samples were centrifuged at $717 \times g$ for 10 min at room temperature. Each particle suspension was measured against a blank, PBS negative control, and 1% Triton-X 100 positive control. The amount of hemoglobin released into the supernatant was determined spectrophotometrically at a wavelength of 540 nm, similar to the methods reported by Duffin *et al.* (2001).

Statistical Analyses

For analyses, each of the experimental values were compared to their corresponding PBS control values for each time point. A one-way analysis of variance (ANOVA) and Bartlett's test were calculated for each sampling time. When the F -test from ANOVA was significant, the Dunnett's test was used to compare means from the PBS control group and each of the groups exposed to particulates. Statistical significance was assessed at the 0.05 probability level.

RESULTS

Physico-chemical Analyses of the α -Quartz Particles

The average particle size and size range, surface area measurements, crystal structures, and purity (including iron content) for the various α -quartz particles are presented in Figure 1 and Table 1. Sizing data were obtained using TEM and scanning electron microscope, as well as DLS spectroscopy. In general, the average particle sizes were inversely correlated with

the surface area measurements. Nanoquartz I particles had an average particle size of 50 nm with a surface area of 31.4 m²/g. Nanoquartz II had an average particle size of 12 nm with a surface area of 90.5 m²/g. Fine quartz had an average particle size of 300 nm with a surface area of 4.2 m²/g. Min-U-Sil had an average particle size of 534 nm with a surface area of 5.1 m²/g (Table 1).

All particle samples clearly demonstrated XRD patterns consistent with crystalline forms of α -quartz. Thermal analyses of nanoquartz I and II further showed the α -quartz purity. The DTA weight loss profile shows loss of residual water at 100°C and < 0.2% burn-off of small molecular weight organic contaminants at 500°C. In addition, ICP-AES analysis of the samples demonstrated minimal iron content: nanoquartz I contained 0.080%, nanoquartz II contained 0.034%, fine quartz contained 0.011%, and Min-U-Sil contained 0.042% (Fig. 1 and Table 1).

Experiment #1 [Min-U-Sil and Nanoquartz I Samples]

BAL Fluid Results

Pulmonary inflammation. The numbers of cells recovered by BAL from the lungs of high-dose Min-U-Sil quartz-exposed (5 mg/kg) groups were substantially higher than any of the other groups for all pe time periods (Fig. 2). Intratracheal instillation exposures to high-dose nanoquartz I particle produced a substantial lung inflammatory response at 24 h pe followed by a minimal but sustained recruitment of neutrophils (i.e., 15–20% polymorphonuclear leukocytes for pe time points through 3 months). In contrast, intratracheal instillation exposures to Min-U-Sil quartz particles (1 and 5 mg/kg) produced persistent pulmonary inflammatory responses, with the high dose producing > 40% neutrophils through 3 months pe (Fig. 2).

BAL fluid parameters. Slight but significant increases in BAL fluid LDH values versus PBS controls were measured in the lungs of rats exposed to the high dose (5 mg/kg) of nanoquartz I particles and were sustained through the 3-month pe time period. Similarly, small but significant increases in BAL fluid microprotein values were measured at 24 h and 1 week pe. In contrast, exposures to 5 mg/kg Min-U-Sil quartz particles produced a persistent and progressive increase in BAL fluid LDH and microprotein values throughout the 3-month pe period (Fig. 3).

Experiment #2 [CI, Min-U-Sil, Nanoquartz II and Fine-Quartz Samples]

BAL Fluid Results

Pulmonary inflammation. The numbers of cells recovered by BAL from the lungs of high-dose Min-U-Sil and nanoquartz II-exposed (5 mg/kg) groups were substantially higher compared to CI, fine-quartz particle or PBS-exposed groups for all

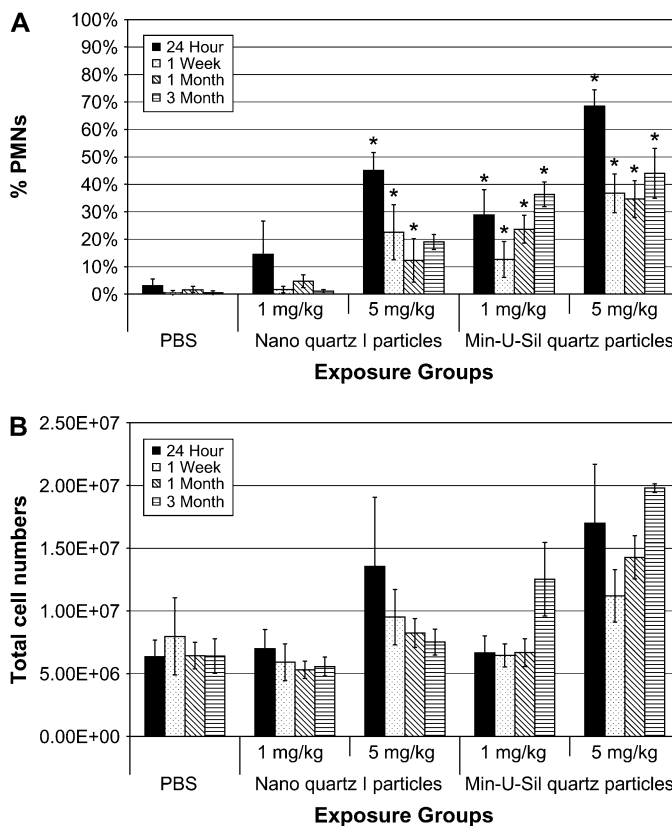


FIG. 2. Total cell numbers and percent neutrophils in BAL fluids of rats exposed to nanoquartz I and Min-U-Sil particles. The (A) total cell numbers and (B) percent neutrophils in BAL fluids of rats exposed to nanoquartz I and Min-U-Sil particles. Data were taken at 24-h, 1-week, 1-month, and 3-months. *Indicates statistical significance ($p > 0.05$).

pe time periods (Fig. 4). Intratracheal instillation exposures to Min-U-Sil or nanoquartz II particles (1 and 5 mg/kg) produced persistent pulmonary inflammatory responses, with the high dose producing in the range of 40% neutrophils through 3 months pe (Fig. 4). Exposures to high-dose, fine-quartz particles produced a reduced inflammatory response when compared to Min-U-Sil or nanoquartz II samples.

BAL fluid parameters. Exposures to 5 mg/kg Min-U-Sil or nanoquartz II particles produced persistent and progressive increases in BAL fluid LDH and microprotein values throughout the 3-month pe period (Fig. 5). Slight increases in BAL fluid LDH values versus PBS controls were measured in the lungs of rats exposed to the high-dose (5 mg/kg) fine-quartz particles and were not significantly different versus PBS through the 3-month pe time period. CI particle exposures produced no significant effects.

To summarize the results from BAL fluid biomarker studies, for both experiments, pulmonary exposures to Min-U-Sil quartz particles produced sustained, dose-dependent, lung inflammatory responses, concomitant with cytotoxic effects, measured from 24 h through 3 months pe. Exposures to

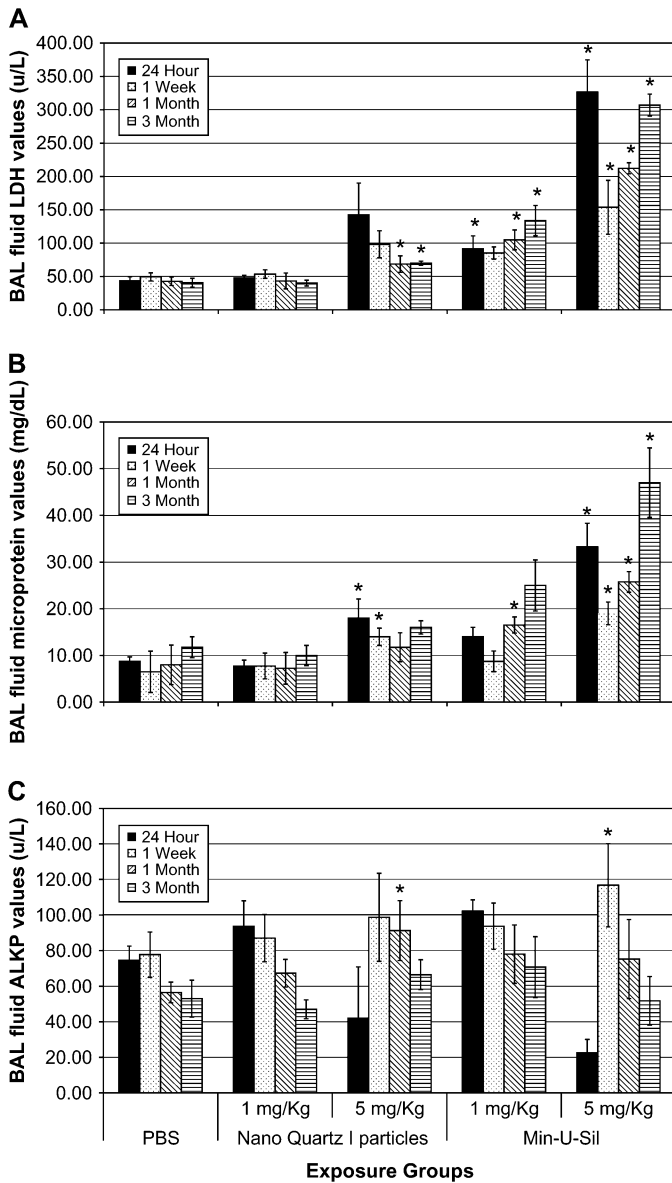


FIG. 3. BAL fluid biochemical endpoints in rats exposed to nanoquartz I and Min-U-Sil particles. The cytotoxicity endpoints from the nanoquartz I study. (A) LDH, (B) micro total protein (MTP), and (C) ALKP values in BAL fluids of rats exposed to nanoquartz I and Min-U-Sil particles. Data was taken at 24-h, 1-week, 1-month, and 3-month time points. *Indicates statistical significance ($p > 0.05$).

nanoquartz I particles produced a potent initial inflammatory response but was followed by a less than moderate response at the other pe time periods. In the second experiment, exposures to nanoquartz II particles produced persistent lung inflammatory responses, similar to Min-U-Sil quartz particles. In addition, the neutrophilic and cytotoxic responses to fine quartz generally were lower in intensity when compared to Min-U-Sil quartz or nanoquartz II particles, as well as nanoquartz I particles.

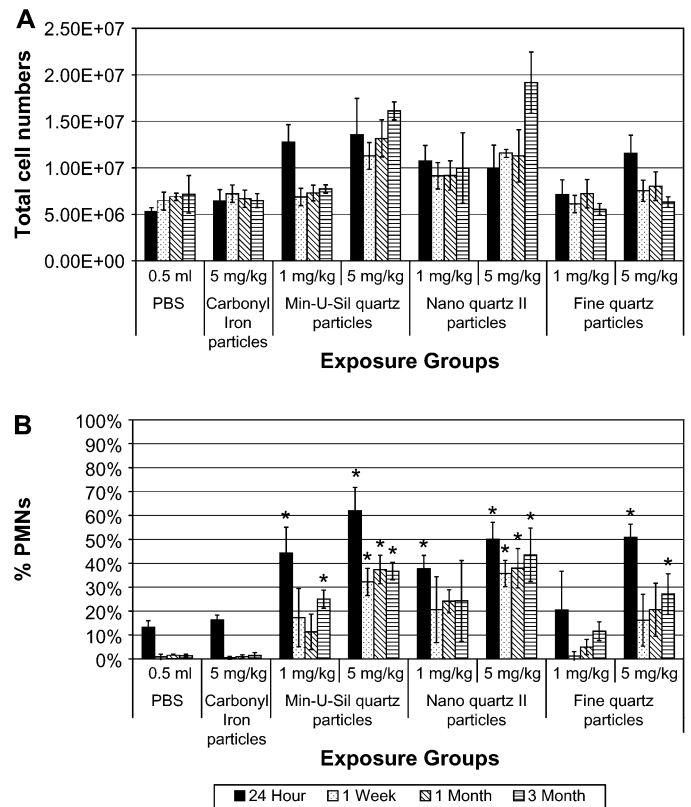


FIG. 4. Total cell numbers and percent neutrophils in BAL fluids of rats exposed to Min-U-Sil, nanoquartz II, and fine-quartz particles. The (A) total cell numbers and (B) percent neutrophils in BAL fluids of rats exposed to Min-U-Sil, nanoquartz II, and fine-quartz particles. Data were taken at 24-h, 1-week, 1-month, and 3-month time points. *Indicates statistical significance ($p > 0.05$).

Lung tissue studies. Lung tissue studies were conducted with particle types evaluated in Experiment #2.

Lung weights. Lung weights of rats were increased with increasing age on the study (i.e., increased pe time periods following instillation). Lung weights in high-dose nanoquartz II-exposed rats were slightly increased versus controls at 1 week, 1 month, and 3 months pe. These effects were not significantly different from PBS controls (data not shown).

Cell proliferation results. Tracheobronchial cell proliferation rates (% immunostained cells taking up BrdU) were measured in high dose (5 mg/kg), PBS, CI and fine, nano and Min-U-Sil quartz-exposed rats and corresponding controls at 24 h, 1 week, and 1 and 3 months pe. Transient increases in cell labeling indices were measured in Min-U-Sil quartz-exposed (1 and 5 mg/kg) as well as in high-dose nanoquartz II-exposed animals at 24 h pe, but these effects were not sustained (Fig. 6).

Lung parenchymal cell proliferation rates (% immunostained cells taking up BrdU) were measured in high dose (5 mg/kg), CI, along with fine, nano II and Min-U-Sil quartz-exposed rats and PBS controls at 24 h, 1 week, and 1 and 3 months pe. Significant increases in cell labeling indices versus PBS

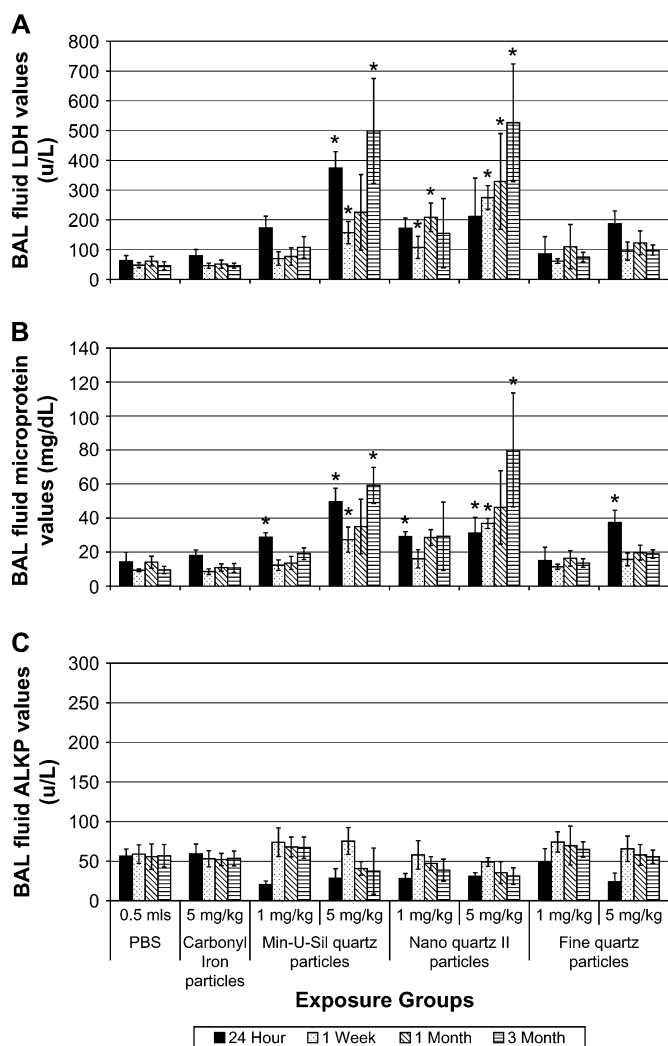


FIG. 5. BAL fluid biochemical endpoints in rats exposed to Min-U-Sil, nanoquartz II, and fine-quartz particles. The cytotoxicity endpoints from the nanoquartz II study. (A) LDH, (B) micro total protein (MTP), and (C) ALKP values in BAL fluids of rats exposed to Min-U-Sil, nanoquartz II, and fine-quartz particles. Data were taken at 24 h, 1 week, 1 month, and 3 month postinstillation exposure. *Indicates statistical significance ($p > 0.05$).

controls were measured in high-dose Min-U-Sil and nanoscale quartz II-exposed animals at 24 h and 1 week pe, but these effects were not sustained through 1 and 3 months pe (Fig. 6).

To summarize the results of airway and alveolar cell proliferation studies, when compared to other particle types such as CI or fine quartz, or PBS controls, pulmonary exposures to 5 mg/kg Min-U-Sil or nanoscale quartz II particles produced higher lung parenchymal cell proliferation rates at 24 h and 1 week pe.

Histopathological evaluation. Histopathological analyses of lung tissues revealed that pulmonary exposures to CI particles produced no significant adverse effects when compared to PBS-exposed controls; as evidenced by the normal lung architecture observed in the exposed animals at post-

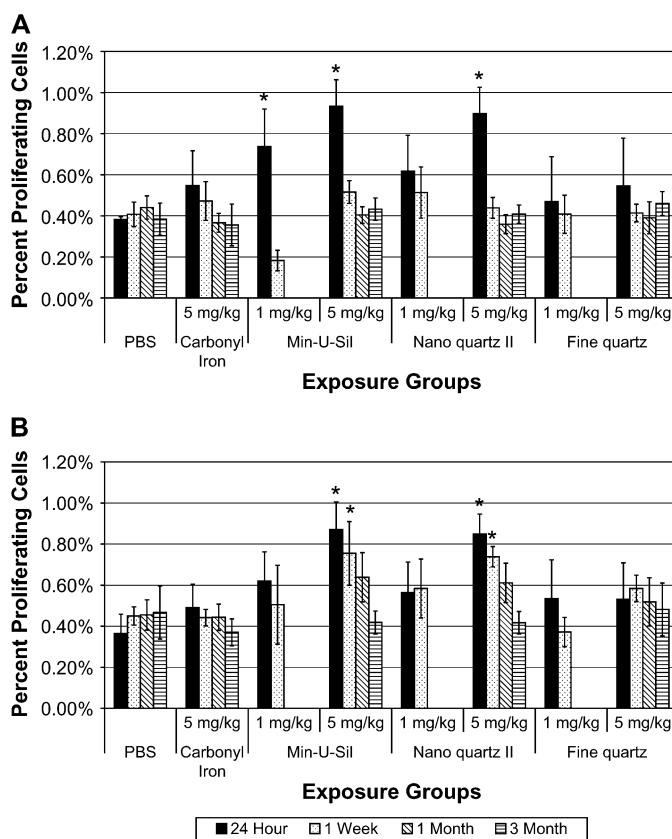


FIG. 6. Tracheobronchial epithelial and lung parenchymal cell proliferation rates of rats exposed to Min-U-Sil, nanoquartz II, and fine-quartz particles. (A) Tracheobronchial epithelial and (B) lung parenchymal cell proliferation rates of rats exposed to Min-U-Sil, nanoquartz II, and fine-quartz particles. Data were taken at 24-h, 1-week, 1-month, and 3-month time points. *Indicates statistical significance ($p > 0.05$).

instillation exposure time periods ranging from 24 h to 3 months (Fig. 7A).

Histopathological analyses of lung tissues revealed that pulmonary exposures to Min-U-Sil quartz (Fig. 7B), nanoquartz II particles (Fig. 7C), or fine quartz (Fig. 7D) in rats all produced dose-dependent lung inflammatory responses characterized by the recruitment of neutrophils, concomitant with foamy (lipid-containing) alveolar macrophage accumulation and progressive lung tissue thickening. In general, these effects were observed at or near the junctions of the terminal bronchioles and alveolar ducts, although some of these processes were observed in subpleural regions. It is important to note that the patterns and characteristics of lung histopathological effects in responses to nanoquartz II, Min-U-Sil quartz, or fine-quartz particles were virtually identical (i.e., inflammation, foamy alveolar macrophage accumulation, lung tissue thickening). However, from a potency standpoint, the degree and extent of involvement of these processes within the alveolar structures was evident most frequently and substantially in the lungs of nanoquartz II or Min-U-Sil quartz-exposed rats at 1 and 3 months pe (Fig. 7B and 7C) and less frequently in the lungs of fine-quartz-exposed rats (Fig. 7D).

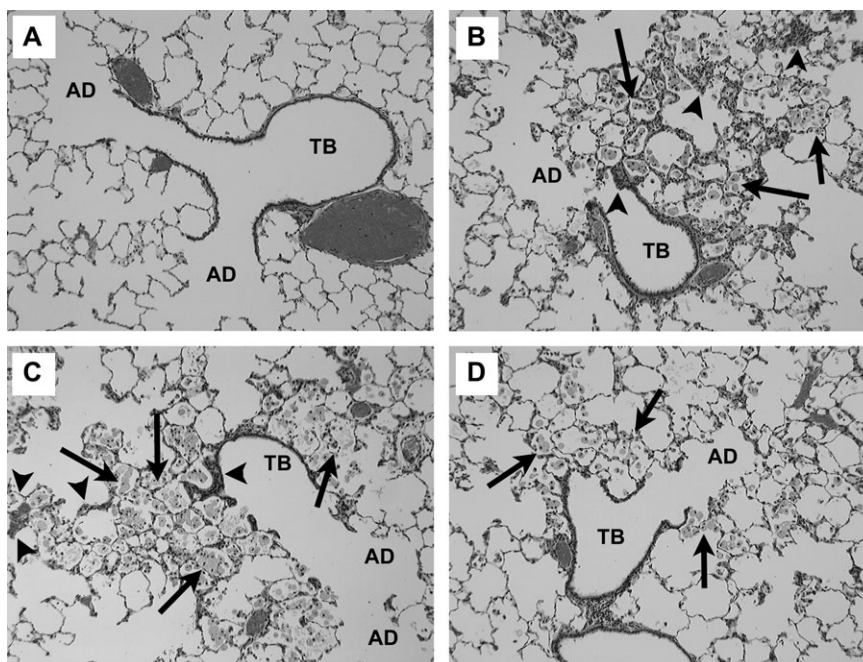


FIG. 7. Light micrograph of lung tissue from rats exposed to particles (5 mg/kg) at 3 months postinstillation exposure. Each micrograph illustrates the terminal bronchial (TB) and corresponding alveolar ducts (AD). (A) CI particles: Demonstrates normal lung architecture following CI exposures. (B) Min-U-Sil quartz particles: the tissue accumulation of foamy alveolar macrophages (arrows) within alveolar spaces. (C) Nanoquartz II: the tissue accumulation of foamy alveolar macrophages (arrows) within alveolar spaces. (D) Fine-quartz particles: the tissue accumulation of foamy alveolar macrophages (arrows) within alveolar spaces. For graphs B–D, the macrophages have migrated to the sites of quartz particle instillation at the terminal bronchiolar alveolar junctions. The accumulation of lipid-filled macrophages, lack of clearance, and development of tissue thickening (arrowhead) are common features of the progressive nature of silica-induced lung disease (magnification = $\times 100$).

Semiquantitative morphometric evaluation of lung tissue at 3 months pe revealed that 15 and 18 BA junctions, respectively, were identified in lung tissue sections from PBS and CI-exposed rats. No evidence of macrophage accumulation or tissue thickening was observed in any of those sections. Assessments of BA junctions from fine-quartz-exposed rats indicated that 8 of 15 lung sections demonstrated evidence of macrophage accumulation, and early fibrosis was observed in 5 of 15 sections. Evaluations of BA junctions from Min-U-Sil and Nanoquartz II-exposed lung tissue sections revealed that of 22 BA junctions in Min-U-Sil quartz-exposed rats, 20 sections contained accumulations of foamy macrophages and 17 had evidence of thickening; for nanoquartz II samples, of 21 BA sections evaluated, 19 contained accumulated macrophages and early fibrosis was noted in 18 lung sections.

ESR spectra for determination of radical species. The ESR spectrum of mined Min-U-Sil was dramatically different from the spectra of synthetic quartz particles. The spectrum of Min-U-Sil contains similar peaks as reported by Fubini (1998) and Clouter *et al.* (2001). The g -factors of 2.015, 2.000, and 1.98 are all present in the Min-U-Sil sample used in these studies and correspond to SiO_2^\bullet , O_2^\bullet , and Si^\bullet , centered radical species, respectively. However, the nanoquartz I, nanoquartz II, and fine-quartz particle samples only contain a peak at $g = 2.080$.

Accordingly, it was concluded that the ESR spectra for the various α -quartz samples did not correlate with pulmonary responses in exposed rats (data not shown).

Hemolytic potential of α -quartz particles. Results from the hemolytic potential assay demonstrated the differential surface activity of each α -quartz sample when incubated with RBC. Data are represented as the absorbance intensity of hemoglobin released into solution versus concentration of the α -quartz sample tested. Each particle suspension was measured against a blank, PBS negative control, and 1% Triton-X 100 positive control. Graphical analysis showed a trend that correlated with inflammation, cytotoxicity, and cell proliferation data, i.e., nanoquartz II = Min-U-Sil > fine quartz > nanoquartz I (Fig. 8). Accordingly, it appears likely that, for this study, the hemolytic surface activity results provided the best correlation with the data generated from the pulmonary bioassay studies, when compared to other characteristics such as particle size, surface area, iron content, crystallinity, or ESR measurements (Table 2).

DISCUSSION

The objective of this pulmonary bioassay study was to assess the relationship between particle size/surface area and/or

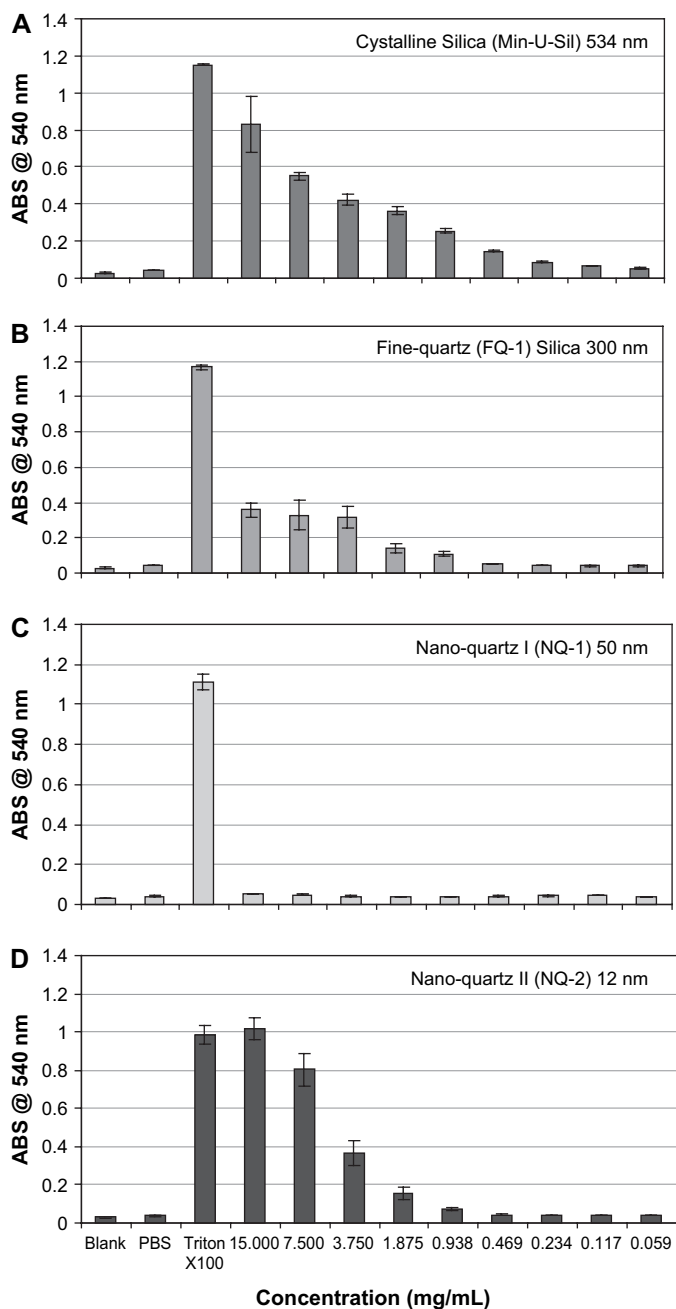


FIG. 8. Hemolytic potential of α -quartz particles. The hemolytic potential of the α -quartz particles used in the study. Data are plotted as absorbance intensity at 540 nm (the intensity of hemoglobin released into solution) versus concentration. Each particle suspension was measured against a blank, PBS negative control, and 1% Triton-X 100 positive control. The samples, including (A) Min-U-Sil, (B) fine quartz, (C) nanoquartz I, and (D) nanoquartz II, show the same trend as the inflammation, cytotoxicity, and cell proliferation data, i.e., nanoquartz II = Min-U-Sil > fine-quartz > nanoquartz I.

surface activity with acute lung toxicity endpoints of intratracheally instilled, well-characterized nanoscale, and fine-quartz particle types in rats. Using pulmonary bioassay methodology, the lung toxicity of intratracheally instilled

TABLE 2
Summary of α -Quartz Results

Endpoint	Min-U-Sil	Nanoquartz I	Nanoquartz II	Fine quartz
Particle size	++++	++	+	+++
Surface area	+	+++	++++	++
Fe content	++	+++	++	+
Crystallinity	++++	++++	++++	++++
Radical content	++++	++	+++	-
Hemolytic potential	+++	+	+++	++
Lung inflammation	+++	++	+++	++
Cytotoxicity	+++	++	+++	+
Airway BrdU	++	NA	++	+
Lung parenchymal BrdU	++	NA	++	+
Histopathology	+++	NA	++++	++

Note. The table summarizes the results of the study. The range of particle-related toxicities and histopathology in descending order were nanoscale quartz II = Min-U-Sil quartz > fine quartz > nanoscale quartz I > CI particles. In this study, the hemolytic surface activity results provided the best correlation with the data generated from the pulmonary bioassay studies, when compared with particle size, surface area, iron content, crystallinity, or ESR measurements. Within the table, ++++ indicates the greatest value, where + indicates the least value. NA stands for data not available.

nanoscale or fine-quartz samples were compared with a positive control particle type, Min-U-Sil 5 α -quartz particles, as well as with a negative control particle type, CI particles. Exposures to CI particles or to the vehicle, PBS, resulted in short-term and reversible lung inflammation (at 24 h); likely related to the effects of the instillation procedure, with the longer term pe time points producing no significant adverse pulmonary effects. Results from the BAL fluid and cell proliferation evaluations demonstrated that pulmonary exposures to all forms of α -quartz particle types, regardless of particle size, produced significant adverse effects versus controls in pulmonary inflammation and cytotoxicity indices. Histopathological evaluations revealed that exposures to all forms of α -quartz particles tested produced pulmonary inflammation, foamy macrophage accumulation, and tissue thickening (i.e., fibrosis). However, the intensity and scope/distribution of adverse pulmonary effects related to the various forms of α -quartz particle types were variable and not dependent on particle size. The toxicity range of lung inflammation/cytotoxicity/cell proliferation and histopathological responses were, in descending order, nanoscale quartz II = Min-U-Sil quartz > fine quartz > nanoscale quartz I > CI particles. It is noteworthy that the toxicity range for the various α -quartz particle types correlated directly with the results of hemolytic potential experiments (see Table 2). It has been suggested that the hemolysis caused by silica particles is partly related to the formation of H_2O_2 at the particle surface (Razzaboni and Bolsaitis, 1990). Thus, it is concluded that the potency of lung toxicity effects of quartz particle types appears to be more dependent upon particle surface activity effects rather than particle size and surface area.

Donaldson and colleagues have conducted numerous studies investigating the lung toxicological effects of various quartz samples. These investigators have concluded that the pulmonary toxicity of quartz particles is a variable entity, meaning that the surface reactivities of different quartz particulates samples are so variable that these differences in activities of different quartz particle types preclude drawing any general conclusions regarding the toxicity of quartz. In this regard, Donaldson and coworkers noted that many of the toxicity studies conducted with quartz have utilized standard active reference samples (DQ12 in Europe; Min-U-Sil in North America). These samples serve as "positive control reference particulates" in many experiments, due, in large part, to the fact that pulmonary exposures in rats to either of these two quartz particle types have always produced sustained and progressive inflammatory responses, i.e., corresponding lung fibrosis as a prerequisite for the development of lung tumors (Donaldson and Borm, 1998; Donaldson *et al.*, 2001a; Duffin *et al.*, 2001).

In support of this notion, Clouter *et al.* (2001) postulated that workplace quartz samples would differ in toxicity from standard experimental DQ12 quartz samples at equivalent doses. Accordingly, these investigators compared two workplace quartz samples with reference DQ12 particulates, utilizing several different toxicity-based assays. The endpoints of this study were the following: release of soluble iron from particles, *in vitro* cytotoxicity biomarkers, inflammation in the rat lung following intratracheal instillation, and surface activity as assessed by hemolytic potential and ESR. Results demonstrated that the workplace samples did not cause inflammation at any dose or time point. DQ12 quartz particles caused marked inflammatory responses, as measured by increased inflammation and permeability in the lungs of instilled animals for both time points and doses measured. *In vitro*, DQ12 had the greatest hemolytic activity but only one of the two workplace quartz samples released substantial amounts of soluble iron. The authors concluded that the enhanced inflammogenicity of DQ12 particulates was not wholly explained by a greater surface area, by diameter, or by releasable iron. It was noteworthy that the hemolytic activity of DQ12 was considered to be the best *in vitro* predictor for *in vivo* activity. Thus, it was noted by these investigators that the surface activity of DQ12 appeared to strongly influence its inflammogenic potential (Clouter *et al.*, 2001).

Hemolytic Potential of α -Quartz Particles

Similar to the studies of Clouter *et al.* (2001), the ESR data did not correlate with pulmonary endpoints. However, the results of hemolytic assay studies demonstrated a toxicity trend that was commensurate with pulmonary lung inflammation results. Nanoquartz II and Min-U-Sil particles lysed the RBC at similar rates (intensity/concentration). Nanoquartz I particle types did not lyse the RBC at any concentration (up to 15 mg/

ml). The mechanism through which the RBC are lysed is reported to be either surface activity related (either defect sites or jagged edges along the crystal facets) or ease in producing reactive species (Razzaboni and Bolsaitis, 1990). The definitive answer is probably due to a synergy between these two theories. Further experiments with fresh nanoparticles need to be conducted to specifically address the surface activity of α -quartz particles. Nonetheless, it has been known for at least two decades that α -quartz is a potent hemolytic agent in RBC systems. The hemolytic effects appear to be related to the quartz surface and the erythrocyte cell interaction, i.e., the active site on the particle is considered to be associated with the silanol group and its proclivity to donate hydrogen ions. The surface of the quartz is hydrated in the presence of water to form a silanol group, which imparts functionalities available for bonding (Nolan *et al.*, 1981). However, the relationship of hemolytic potential with erythrocytes relative to inflammation in the lung still remains to be elucidated. Fubini (1998) has suggested that surface radicals and iron-derived reactive oxygen species are associated with the development of oxidative stress, which leads to inflammation and fibrosis in the lung.

It is interesting to note that the results presented herein are consistent with the findings of Clouter *et al.* (2001) who reported considerable differences in toxicity between workplace quartz samples when compared to reference DQ12 quartz particle types utilized in experimental studies. It was noteworthy that DQ12 particle types had the greatest hemolytic activity of all of the samples tested. These investigators concluded that since the hemolytic activity of DQ12 was the best *in vitro* predictor for *in vivo* activity, the surface activity of DQ12 appears to drive its inflammogenicity (Clouter *et al.*, 2001). In our study, we compared the pulmonary toxicity of four different quartz samples of varying particle sizes, including two nanoscale α -quartz samples, using a pulmonary bioassay methodology in rats. Although all of the instilled quartz samples produced ongoing inflammation and adverse lung effects, the potency range of toxicity was not correlated with particle size and surface area, but was consistent with the results of *in vitro* erythrocyte hemolysis studies. Therefore, from a hazard standpoint, similar to the results reported by Clouter *et al.* (2001), it is concluded that the pulmonary toxicity of α -quartz particles appears to be related to the surface activity of the quartz particle types.

ACKNOWLEDGMENTS

This study was supported by DuPont Central Research. Elizabeth Wilkinson and Denise Hoban conducted the BAL fluid biomarker assessments and hemolytic potential experiments. Carolyn Lloyd, Lisa Lewis, John Barr prepared lung tissue sections and conducted the BrdU cell proliferation staining methods. Don Hildabrandt provided animal resource care. We thank Alex Marchione and Dr. Lloyd Abrams for carrying out ESR and particle size

studies, respectively, and to Drs. Brian Coleman and Gerald L. Kennedy, Jr. for helpful comments on this manuscript.

REFERENCES

- Brunauer, S., Emmett, P. H., and Teller, E. (1938). Adsorption of gases in multimolecular layers. *J. Am. Chem. Soc.* **60**, 309–319.
- Clouter, A., Brown, D., Hohr, D., Borm, P., and Donaldson, K. (2001). Inflammatory effects of respirable quartz collected in workplaces versus standard DQ12 quartz: Particle surface correlates. *Toxicol. Sci.* **63**, 90–98.
- Donaldson, K., and Borm, P. J. A. (1998). The quartz hazard: A variable entity. *Ann. Occup. Hyg.* **42**, 287–294.
- Donaldson, K., Stone, V., Duffin, R., Clouter, A., Schins, R., and Borm, P. (2001a). The quartz hazard: Effects of surface and matrix on inflammogenic activity. *J. Environ. Pathol. Toxicol. Oncol.* **20** (Suppl. 1), 109–118.
- Donaldson, K., Stone, V., Clouter, A., Renwick, L., and MacNee, W. (2001b). Ultrafine particles. *Occup. Environ. Med.* **58**, 211–216.
- Duffin, R., Gilmour, P. S., Schins, R. P., Clouter, A., Guy, K., Brown, D. M., MacNee, W., Borm, P. J., Donaldson, K., and Stone, V. (2001). Aluminium lactate treatment of DQ12 quartz inhibits its ability to cause inflammation, chemokine expression, and nuclear factor-kappa B activation. *Toxicol. Appl. Pharmacol.* **176**, 10–17.
- Fubini, B. (1998). Surface chemistry and quartz hazard. *Ann. Occup. Hyg.* **42**, 521–530.
- Harington, J. S., Macnab, G. M., Miller, K., and King, P. C. (1971). Enhancement of haemolytic activity of asbestos by heat-labile factors in fresh serum. *Med. Lav.* **62**, 171–176.
- Nolan, R. P., Langer, A. M., Harington, J. S., Oster, G., and Selikoff, I. J. (1981). Quartz hemolysis as related to its surface functionalities. *Environ. Res.* **26**, 503–520.
- Oberdorster, G., Oberdorster, E., and Oberdorster, J. (2005). Nanotoxicology: An emerging discipline evolving from studies of ultrafine particles. *Environ. Health Perspect.* **113**, 823–839.
- Otwinowski, Z., and Minor, W. (1997). *Macromolecular Crystallography, Pt A*, Vol. 276, pp. 307–326. Academic Press Inc., San Diego, CA.
- Razzaboni, B. L., and Bolsaitis, P. (1990). Evidence of an oxidative mechanism for the hemolytic activity of silica particles. *Environ. Health Perspect.* **87**, 337–341.
- Warheit, D. B., Carakostas, M. C., Hartsky, M. A., and Hansen, J. F. (1991). Development of a short-term inhalation bioassay to assess pulmonary toxicity of inhaled particles: Comparisons of pulmonary responses to carbonyl iron and silica. *Toxicol. Appl. Pharmacol.* **107**, 350–368.
- Warheit, D. B., Hansen, J. F., Yuen, I. S., Kelly, D. P., Snajdr, S., and Hartsky, M. A. (1997). Inhalation of high concentrations of low toxicity dusts in rats results in pulmonary and macrophage clearance impairments. *Toxicol. Appl. Pharmacol.* **145**, 10–22.
- Warheit, D. B., Webb, T. R., Sayes, C. M., Colvin, V. L., and Reed, K. L. (2006). Pulmonary instillation studies with nanoscale TiO₂ rods and dots in rats: Toxicity is not dependent upon particle size and surface area. *Toxicol. Sci.* **91**, 227–236.